

The Physical and Numerical Implications of the Noise Modeling Method: IFM, CPM, and ERS

Hyunchul Nah, Sung-min Hong, Young June Park*, and Hong Shick Min

School of Electrical Engineering and Computer Science and Inter-University Semiconductor Research Center (ISRC),

Seoul National University, Seoul 151-744, Republic of Korea

*Email: ypark@snu.ac.kr, Telephone: 82-2-880-7285, Fax.: 82-2-882-4658

Abstract—In this paper, several aspects of the numerical methods for the noise modeling are introduced such as the impedance field method, the characteristic potential method, and the extended Ramo-Shockley theorem and their implications are discussed. The challenges faced in the $1/f$ noise modeling of MOSFETs and suggestions for the direction of the noise modeling are also discussed.

I. INTRODUCTION

As the noise of the semiconductor devices is regarded as one of the limiting factors of the device scaling in VLSI circuits, its modeling and prediction under the scaled processes and device parameters become more important.

However, the numerical modeling society does not seem to respond to its need as it has done to understanding of the dopant distribution and carrier dynamics and statics. One of the reasons is the lack of the thorough understanding of the noise behavior and interactions with the process parameters such as the defect density of the oxide versus the Hooge parameter α in the $1/f$ noise of MOSFETs.

In this paper, several aspects of the numerical methods for the noise modeling and the advancement of the $1/f$ noise modeling of MOSFET from our group will be introduced, which are followed by some suggestions for the direction of the noise modeling.

II. IFM, CPM, AND THE EXTENDED RAMO-SHOCKLEY THEOREM

The numerical modeling of the noise of the semiconductor devices requires the understanding of randomness of the carrier dynamics at a local point and its effects on the device terminals in the form of the voltage or the current fluctuations.

In the moment approach of the Boltzmann transport equation, the spontaneous local fluctuations can be represented by the Langevin sources in the continuity equations for the carrier density, average velocity, energy, and the energy flux [1]. In the Monte Carlo (MC) simulation, the spontaneous fluctuations can be obtained self-consistently, where the sources of the fluctuations are embedded in the scattering rates including the recombination rates.

Once the local fluctuations are known, their effects on the terminals can be found by the “transfer functions” introduced in the different hierarchies of the device modeling. In this section, the Green function (GF) [2] in the impedance field method (IFM) [3], the characteristic potential (CP) method [4],

and the extended Ramo-Shockley (RS) method for the MC simulation [5] will be reviewed.

In the GF approach, the fluctuating noise current at the i -th terminal due to the diffusion noise source ξ_α and the associated correlation matrix of the ac-wise short noise current are given as

$$\Delta i_i(\omega) = \sum \int_{\Omega} \mathbf{G}_i^\alpha(\mathbf{r}, \omega) \cdot \xi_\alpha(\mathbf{r}, \omega) d\mathbf{r}, \quad (1)$$

$$S_{\Delta i_i, \Delta i_j}(\omega) = \sum_{\alpha} \int_{\Omega} \mathbf{G}_i^\alpha(\mathbf{r}, \omega) \cdot \mathbf{K}_{\xi_\alpha, \xi_\alpha}(\mathbf{r}, \omega) \cdot \mathbf{G}_j^{\alpha\dagger}(\mathbf{r}, \omega) d\mathbf{r}, \quad (2)$$

where i and j denote the given device terminals, $\mathbf{G}_i^\alpha = \frac{1}{q} \nabla G_i^\alpha$, and G_i^α is the current GF for contact i and carrier α (electrons or holes). $\mathbf{K}_{\xi_\alpha, \xi_\alpha}$ is the microscopic local noise source for velocity fluctuation given as $\mathbf{K}_{\xi_n, \xi_n} = 4q^2 n \mathbf{D}_n$ and $\mathbf{K}_{\xi_p, \xi_p} = 4q^2 p \mathbf{D}_p$.

In the characteristic potential method (CPM) [4], the fluctuation in the current can be obtained by introducing the CP for contact i , ϕ_i , which satisfies

$$\nabla \cdot [(\sigma_s + j\omega\epsilon) \nabla \phi_i] = 0 \quad (3)$$

with the boundary conditions:

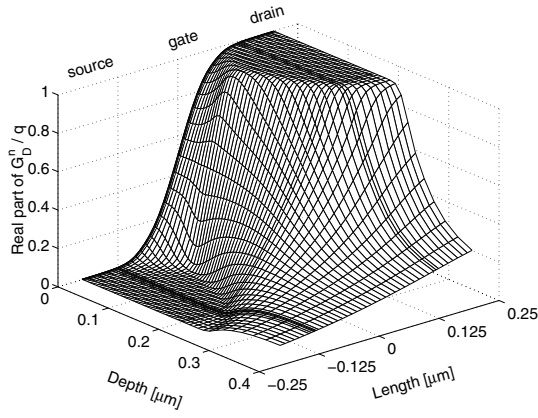
$$\begin{aligned} \phi_i &= 1 \text{ at contact } i \\ \phi_i &= 0 \text{ at other contacts} \\ \mathbf{n} \cdot \nabla \phi_i &= 0 \text{ at free surface.} \end{aligned} \quad (4)$$

Then it can be shown that the noise current flowing through contact i in the ac-wise short condition and the associated correlation matrix of the ac-wise short noise current become

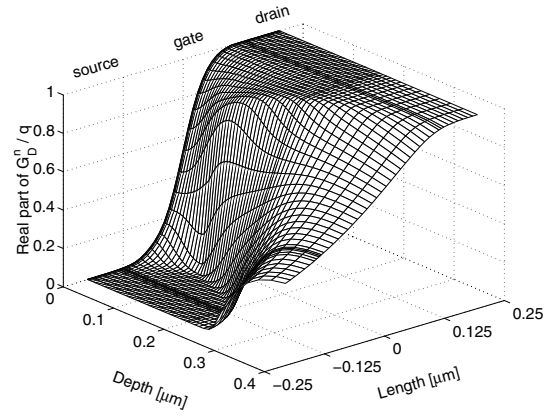
$$\begin{aligned} \Delta i_i(\omega) &= \int_{\Omega} \nabla \phi_i \cdot \left[\xi_{th} + \mathbf{J}_{n_s} \frac{\Delta n}{n_s} + \mathbf{J}_{p_s} \frac{\Delta p}{p_s} \right. \\ &\quad \left. - \sigma_s \nabla \left(\frac{qD_n n_s}{\sigma_s} \right) \frac{\Delta n}{n_s} + \sigma_s \nabla \left(\frac{qD_p p_s}{\sigma_s} \right) \frac{\Delta p}{p_s} \right] d\mathbf{r}. \end{aligned} \quad (5)$$

$$S_{\Delta i_i, \Delta i_j}(\omega) = \sum_{\alpha=th,ex} \int_{\Omega} \nabla \phi_i(\mathbf{r}, \omega) \cdot \mathbf{K}_{\xi_\alpha, \xi_\alpha}(\mathbf{r}, \omega) \cdot (\nabla \phi_j(\mathbf{r}, \omega))^\dagger d\mathbf{r}. \quad (6)$$

The terms related with Δn and Δp are included as an excess noise source(ξ_{ex}) in (6).

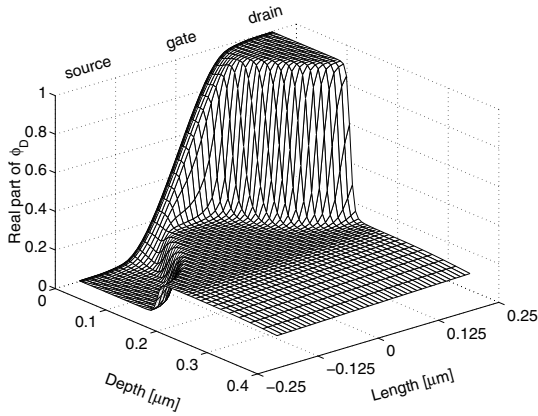


(a)

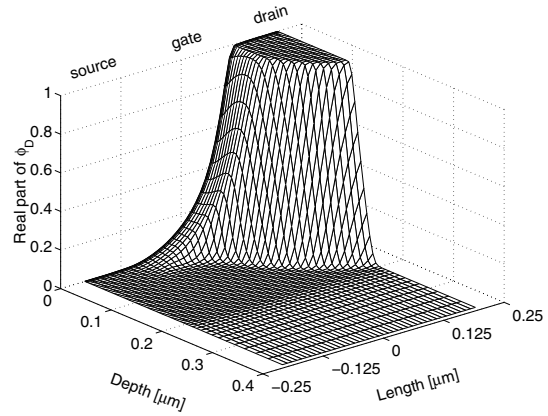


(b)

Fig. 1. Real part of the Green function for the NMOSFET with $L = 0.25 \mu\text{m}$ in (a) linear ($V_{DS} = 0.05 \text{ V}$, $V_{GS} = 1.1 \text{ V}$) and (b) saturation ($V_{DS} = 2.5 \text{ V}$, $V_{GS} = 1.1 \text{ V}$) region. The channel lies between $-0.125 \mu\text{m}$ and $0.125 \mu\text{m}$.



(a)



(b)

Fig. 2. Real part of the characteristic potential for the NMOSFET with $L = 0.25 \mu\text{m}$ in (a) linear ($V_{DS} = 0.05 \text{ V}$, $V_{GS} = 1.1 \text{ V}$) and (b) saturation ($V_{DS} = 2.5 \text{ V}$, $V_{GS} = 1.1 \text{ V}$) region. The channel lies between $-0.125 \mu\text{m}$ and $0.125 \mu\text{m}$.

Comparison of (2) and (6) apparently shows that the CP corresponds to the GF divided by q . It is instructive to understand the differences among CP, GF, and RS. In GF, the influences of the induced terms Δn and Δp are taken into consideration in itself while it is not in the CP and RS. Instead, the CPM treats the induced terms (containing Δn and Δp in (5)) as *a priori* Langevin sources together with the DC solutions. In other words, the CP has advantage of the simpler form of the equation at the expense of the information of the induced Δn and Δp .

The CP helps to eliminate the terms related to the gradients of $\Delta\psi$, Δn , and Δp . In that sense, the CP plays the same role as the RS function, the f in the extended Ramo-Shockley theorem [5], which eliminates the displacement current and makes the instantaneous current at i -th terminal represented

by the instantaneous velocities of the particles as

$$i_i(t) = \int_{\Omega} \nabla f_i(\mathbf{r}) \cdot [qn(\mathbf{r}, t)v_n(\mathbf{r}, t) - qp(\mathbf{r}, t)v_p(\mathbf{r}, t)] d\mathbf{r}. \quad (7)$$

In that sense, the accuracy of the different methods relies on the accuracy of the representation of the fluctuation of the carrier transport equation due to the Langevin source even though the transfer functions may or may not have the effects of the transport equations.

Figs. 1–3 show that the real part of the GF, CP, and RS function for the drain of the NMOSFET with the channel length of $0.25 \mu\text{m}$ operating in the linear region and the saturation region. In the linear region, both the GF and CP have similar properties in the channel. Thus the noise current power spectra obtained by both methods are almost identical. But in the saturation region the CP predicts that the drain region will contribute the dominant effect on the contrary to

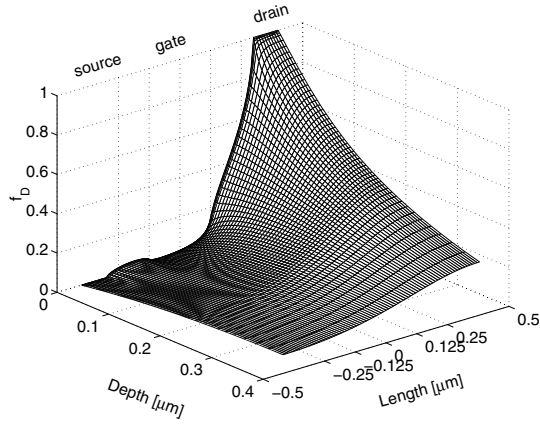


Fig. 3. Ramo-Shockley function for the NMOSFET with $L = 0.25 \mu\text{m}$. The channel lies between $-0.125 \mu\text{m}$ and $0.125 \mu\text{m}$.

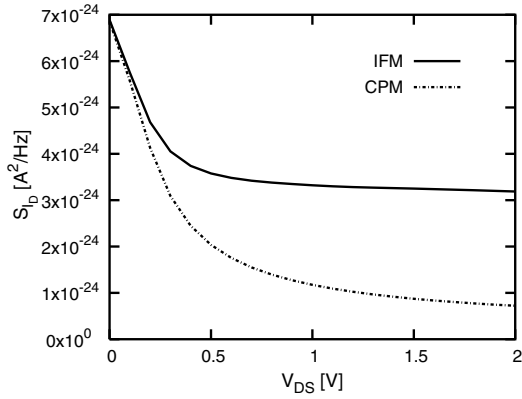


Fig. 4. Numerical simulation based on the IFM and CPM for the drain thermal noise versus V_{DS} for $0.25 \mu\text{m}$ NMOSFET. $V_{GS} = 1.1 \text{ V}$.

the GF (see Fig. 5). As a consequence, the S_{ID} by the CP is far lower than that by the GF (see Fig. 4). It is attributed to the effects of the induced term Δn and Δp and it is expected that if we consider the appropriate induced terms, the two methods may give the same results.

The RS function is quite different especially in the neutral drain region, which implies that the carrier fluctuation is self adjusted in the MC scheme so that the contribution from the neutral drain is minimal.

Also, it should be noticed that the assumption of the relation $G_D^n \simeq 1/L_{eff}$ on which most analytical model rely, is questionable as the channel length decreases as shown in Fig. 5.

III. APPLICATIONS

In this section, the status of the noise modeling of the semiconductor devices will be reviewed in the framework of the three methods introduced in the previous section.

A. $1/f$ noise modeling

Considering ever growing importance of the $1/f$ noise characteristics of MOSFETs, understanding of the method to treat the noise source and the associated formulation of the current equations are required.

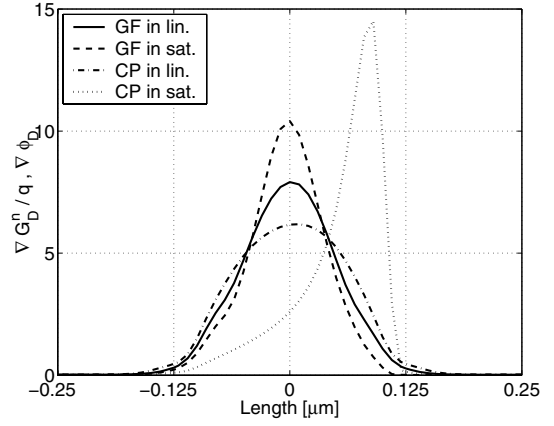


Fig. 5. Gradients of the Green function and the characteristic potential along the channel for $0.25 \mu\text{m}$ device both in the linear and the saturation regions.

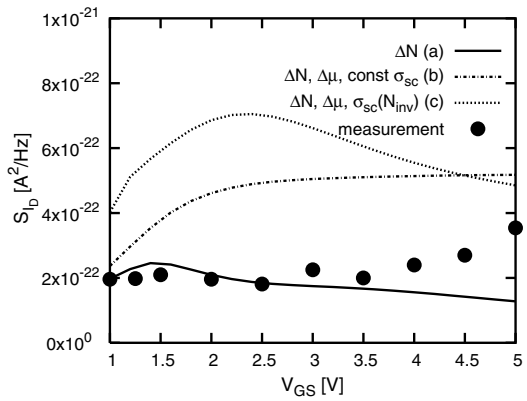


Fig. 6. IFM based numerical simulation for S_{ID} versus gate bias for a long channel ($L = 10 \mu\text{m}$) NMOSFET. $V_T = 0.77 \text{ V}$ and $f = 100 \text{ Hz}$. (a) McWhorter's model [7], (b) McWhorter's model together with the correlated mobility fluctuation using scattering parameter $\sigma_{sc} = 10^{-15} \text{ Vs}$ [6], (c) McWhorter's model together with the correlated mobility fluctuation using $\sigma_{sc} = 1/(5.9 \times 10^8 \sqrt{N_{inv}}) \text{ Vs}$ [8].

The measured power spectral density of the drain current (S_{ID}) normalized by the I_D^2 of MOSFETs operated in the linear region can be written as

$$\frac{S_{ID}}{I_D^2} = \frac{\alpha}{fN_T}, \quad (8)$$

where N_T is the total carrier number in the device and α , called Hooge parameter, is regarded to be related with the physical origin of the noise (fluctuation). Historically, the $V_{GS} - V_T$ dependence of α for PMOSFETs and NMOSFETs has been the guideline to determine the origin of the noise source. In the analytic model, the number fluctuation model based on the McWhorter is used together with the correlated mobility fluctuation due to the random trap charge fluctuation [6]. However, as shown in Fig. 6 from our simulation based on the IFM with the models in [7] and as pointed out in [8], the model cannot predict the correct $V_{GS} - V_T$ dependence for both NMOSFET and PMOSFET unless unphysical fitting parameters are used.

From the power spectrum of the mobility fluctuation repre-

sented as $\frac{S_{\mu}(\mathbf{r}, f)}{\mu^2} = \frac{\alpha(\mathbf{r})}{fn(\mathbf{r})} \delta(\mathbf{r} - \mathbf{r}')$ [9], the power spectrum of ξ_{μ_n} , the source due to the mobility fluctuation $\xi_{\mu_n} = \frac{J_{ns}}{\mu_{ns}} \Delta\mu_n$, is

$$S_{\xi_{\mu_n}} = J_{ns}^2 \frac{\alpha(\mathbf{r})}{fn(\mathbf{r})} \delta(\mathbf{r} - \mathbf{r}'). \quad (9)$$

We believe that the effects of the uncorrelated source as shown in (9) should be included to correctly model the $1/f$ behavior. Despite many efforts have been made for understanding of the relation between α and $\Delta\mu$ [10], the theory for the uncorrelated noise source for mobility is still not satisfactory.

B. Thermal noise modeling

The thermal noise due to the random motion of carrier transport can be modeled using the three methods in Sec. II once the carrier temperature is properly obtained. The γ factor ($\gamma = \frac{S_{ID}}{4k_B T_{qdo}}$) versus V_{DS} is an indicator for the effects of carrier temperature of the velocity saturation regime in the saturation region.

However, the partial success in the prediction of the behavior of γ [11] should be carefully reviewed since the gradient of the GF and CP is far from $1/L_{eff}$ as the channel length is reduced as shown in Fig. 5.

IV. DISCUSSIONS AND SUGGESTIONS FOR THE FURTHER STUDY

A. Local and non-local model

Aside from the physical origins of the noise sources, another problem arises in the numerical implementation of the model. The problem is similar to the mobility model of MOSFETs, where the mobility for $n(x)$, x being the depth direction, should be adjusted in such a way to fit the universal $\mu - \mathcal{E}_{eff}$ relation.

Now, we may have two options in modeling the $\frac{S_{ID}}{I_D^2}$, in order to fit the observed $V_{GS} - V_T$ dependence of $1/f$ noise; the local and the nonlocal model. In the local model, we have to find the correct α (Hooge parameter) value as function of x for electrons and holes to explain the experimental observations. In doing so, we have to find the correct GF or CP to find the proper weight in x direction.

B. The discrete effect: RTN

As the number of data for the oxide related parameters and the noise phenomenon related with the discrete charge effects are accumulated, the numerical simulation communities can utilize the data to enhance the modeling accuracy of the transport models and contribute to understanding of the experimental data. The typical example would be the modeling of the RTS noise, where the current noise is dependent on the trapping and detrapping of the discrete charge in the oxide trap. As the drain current is changed by the localized potential and associated carrier fluctuation, the three dimensional numerical simulation with the proper treatment of the discrete charge and associated mobility fluctuation should be performed to fit the experimental data for various bias and temperature conditions. The experiences can be feedbacked to understanding of the local mobility model and comprehensive study has not been

performed considering the effects of the specific trap (spatial distribution and the energy band) center on the RTS current amplitude. This kind of studies is believed to be one of the ways to expand the capability of numerical simulations of nano-scale CMOS devices.

C. The noise in the cyclostationary condition

The numerical basis for obtaining the effects of the small signal noise on the large signal environment was proposed in [12]. However, the numerical burden prohibits the implementation in the numerical simulator and engineering application. The approach proposed in [13] may be a viable tool to understand the effects of the local fluctuations on the large signal at the terminal.

V. CONCLUSION

Several transfer functions to obtain the effects of the randomness of the carrier dynamics in the device on the terminals have been introduced. The methods based on the IFM, CPM and the extended RS functions are explained and the differences are elucidated.

By showing the $V_{GS} - V_T$ dependence of the $1/f$ noise of MOSFETs with the model using the correlated mobility fluctuation, the need of a new model for the uncorrelated mobility fluctuation is suggested.

The modeling efforts should be given not only to provide the method for the device design for the minimum noise figure, but also to provide new horizons for understanding of the silicon surface and oxide-silicon interface system.

ACKNOWLEDGMENT

The authors appreciate the support of the National Research Laboratory Project of the Ministry of Science and Technology and the Brain Korea 21 Project. This work has also been supported by A Collaborative Project for Excellence in System IC Technology.

REFERENCES

- [1] D. O. Martin, *et al.*, "Impedance field noise simulation of silicon devices operating under DC and AC steady-state conditions," in *Noise and Fluctuations Control in Electronic Devices*, American Scientific Publishers, 2002.
- [2] F. Bonani, *et al.*, *IEEE Trans. ED*, vol. 45, no. 1, p. 261, 1998.
- [3] W. Shockley, *et al.*, "The impedance field method of noise calculation in active semiconductor devices," in *Quantum Theory of Atoms, Molecules, and the Solid-State*; New York: Academic Press, 1966.
- [4] C. H. Park, *et al.*, *J. Phys. D: Appl. Phys.*, vol. 35, p. 637, 2002.
- [5] H. Kim, *et al.*, *Solid-State Electron.*, vol. 34, no. 11, p. 1251, 1991.
- [6] K. K. Hung, *et al.*, *IEEE Trans. ED*, vol. 37, no. 3, p. 654, 1990.
- [7] H. Nah, *et al.*, "A simple 2-D device model for oxide traps as a source of low-frequency noise of MOSFET's," *IEEE Trans. ED*, submitted for publication.
- [8] E. P. Vandamme *et al.*, *IEEE Trans. ED*, vol. 47, no. 11, p. 2146, 2000.
- [9] A. van der Ziel, *Noise in Solid State Devices and Circuits*. New York: John Wiley & Sons, 1986.
- [10] S.-m. Hong, *et al.*, *Proc. SPIE Vol. 5113 Noise in Devices and Circuits*, 2003, p. 267.
- [11] A. J. Scholten, *et al.*, *IEDM Tech. Dig.*, 2002, p. 129.
- [12] F. Bonani, *et al.*, *IEEE Trans. ED*, vol. 50, no. 3, p. 633, 2003.
- [13] K.-I. Lee, *et al.*, *Proc. SISPAD 2003*, 2003.